Lyophilized Silk Fibroin Hydrogels for the Sustained Local Delivery of Therapeutic Monoclonal Antibodies

Nicholas Guziewicz[a], **Annie Best**[a], **Bernardo Perez-Ramirez**[a], and **David L. Kaplan**[b,*]

[a]BioFormulations Development, Genzyme Corporation, 1 Mountain Road, P.O. Box 9322, Framingham, MA 01701-9322

[b]Department of Biomedical Engineering, School of Engineering, Tufts University, 4 Colby St, Medford, MA 02155, USA

Abstract

The development of sustained delivery systems compatible with protein therapeutics continues to be a significant unmet need. A lyophilized silk fibroin hydrogel matrix (lyogel) for the sustained release of pharmaceutically relevant monoclonal antibodies is described. Sonication of silk fibroin prior to antibody incorporation avoids exposing the antibody to the sol-gel transition inducing shear stress. Fourier Transform Infrared (FTIR) analysis showed no change in silk structural composition between hydrogel and lyogel or with increasing silk fibroin concentration. Antibody release from hydrogels occurred rapidly over 10 days regardless of silk concentration. Upon lyophilization, sustained antibody release was observed over 38 days from lyogels containing 6.2% (w/w) silk fibroin and above. In 3.2% (w/w) silk lyogels, antibody release was comparable to hydrogels. Swelling properties of lyogels followed a similar threshold behavior. Lyogels at 3.2% (w/w) silk recovered approximately 90% of their fluid mass upon rehydration, while approximately 50% fluid recovery was observed at 6.2% (w/w) silk and above. Antibody release was primarily governed by hydrophobic/hydrophilic silk-antibody interactions and secondarily altered by the hydration resistance of the lyogel. Hydration resistance was controlled by altering β-sheet (crystalline) density of the matrix. The antibody released from lyogels maintained biological activity. Silk lyogels offer an advantage as a delivery matrix over other hydrogel materials for the slow release of the loaded protein, making lyogels suitable for long-term sustained release applications.

Introduction

The medical importance of monoclonal antibody therapeutics continues to grow. Over 300 such therapeutics are under development and more than 20 are already approved [1]. Antibody based therapies are being developed for a wide range of indications in oncology, immune mediated disorders and wound healing [1,2]. Many of these indications require repetitive dosing lasting anywhere from several weeks to months, and sometimes for the lifetime of the patient [2]. Patient compliance and drug efficacy would be maximized by the development of long-term sustained or localized delivery therapies [3]. Despite these advantages, most protein therapeutics are developed for either intravenous (IV),

*Correspondence to David L. Kaplan. Telephone: +1.617.627.3251; fax: +1.617.627.3231. david.kaplan@tufts.edu..

intramuscular (IM), or subcutaneous (SubQ) administration with bolus dosing. Recombinant human bone morphogenetic protein-2 (rhBMP-2) with a collagen sponge is the only approved implantable protein-matrix combination therapy for local delivery [4,5]. The challenges in manufacturing inherently unstable protein therapeutics are exaggerated if a combination therapy is being developed [6–8]. The availability of versatile and biocompatible sustained delivery matrices that maximize therapeutic protein stability continues to be a significant unmet need.

Biodegradable polymers have been most intensely investigated as possible matrices for sustained release of proteins. The majority of studies have been performed on two types of delivery strategies: micro/nano-spheres and hydrogel-based matrices [9–15]. Both types of matrices have been engineered using synthetic and natural polymers, with the most commonly used synthetic polymers being poly(D,L-lactide-*co*-glycolide) (PLGA), and poly(vinyl alcohol) (PVA) [9,16–17]. The material properties of synthetic polymers can be customized by controlling the composition of monomers, altering polymerization conditions, or introducing functional groups [18]. Maintaining protein stability during encapsulation in these synthetic polymers has been problematic due to significant differences in hydrophobicity and unfavorable microclimates caused by degradation products [6,7,18,19]. Natural polymers that have been studied for protein release include collagen, gelatin, fibrin, hyaluronic acid, chitosan and alginate [20]. Natural polymers have the advantage of typically being biocompatible and biodegradable, but batch to batch variability and a more limited range of physical properties can be restrictive [20].

Tolerance of hydrogels by living tissue and compatibility with bioactive agents such as cells and proteins have contributed to their popularity as biomaterials [13,21,22]. Hydrogels are created by the cross-linking of polymer chains, leading to the creation of a three dimensional, structurally integral, hydrophilic matrix [8,13]. Hydrogel constructs have been used for protein delivery as is, in the hydrated state, or they have been dehydrated through air drying or lyophilization, and subsequently rehydrated for use [5,23,24]. Sustained release from hydrogels is characterized by a rate-limiting step which can be diffusion-based or swelling-based [8]. Diffusion of drugs is not typically retarded to a significant degree in the swollen state of a hydrogel, as the typical mesh sizes for hydrogels range from 5 to 100 nm [8]. Therefore, hydrophilic and rapidly swelling hydrogels are limited in sustained release capabilities, making them suitable for short-term but not mid- or long-term release needs.

Cross-linked hydrogels can be produced through chemical agents [25,26]. This strategy is generally not compatible with entrapped proteins due to chemical modifications and loss of bioactivity. The collagen sponge used for rhBMP-2 delivery is chemically cross-linked in the absence of protein, and then adsorbs the rhBMP-2 solution in the operating room at the point of use [4,5]. Hydrogels can also be produced by physical cross-linking through repetitive peptide or polymer segments via hydrophobic/hydrophilic interactions [8]. This approach avoids the use of harsh chemical treatments, and can be more compatible with fragile protein therapeutics.

Silk fibroin is a natural protein that physically cross-links into hydrogel matrices [27,28]. Silk fibroin consists of disulfide bound heavy and light chains of ~370 kDa and ~25 kDa, respectively [29]. The primary structure consists of 12 hydrophobic protein domains rich in alanine and glycine residues with a high propensity towards forming anti-parallel β-sheet (physical cross links) structure. These blocks are separated by 11 small hydrophilic amorphous domains. Silk fibroin possesses useful features as a biomaterial, including a history of biocompatibility, an all aqueous manufacturing process, controllable degradation rates and impressive mechanical properties [30–33]. Specifically, silk fibroin materials have demonstrated favorable immunological properties, a critical consideration when implanting

protein-based materials [30,34–36]. Silk gel formation can be induced by several methods such as pH, temperature, shear, vortexing, electricity and sonication [27,28,33,37,38]. The use of silk-based biomaterials to stabilize and release proteins has been reported [39,40]. These studies revealed that proteins incorporated into silk films in trapped or untrapped forms. Untrapped protein interacted with silk in a reversible manner, releasing rapidly from the matrix, while in the trapped form irreversible interactions were found that required degradation of the silk matrix for release.

A new sustained delivery matrix, a lyogel, was produced by the lyophilization of antibody-loaded silk hydrogels. The goal of the present work was to study the interactions between antibodies and lyogels to determine feasibility as a potential protein therapeutic delivery system. A murine monoclonal antibody was used as a pharmaceutically relevant model protein to assess entrapment and sustained release from silk lyogels. Sonication in the absence of antibody was utilized to induce hydrogel formation due to the method's potential for compatibility with fragile protein therapeutics [37]. The impact of lyophilization was evaluated by comparing antibody release rates between lyogels and the parent hydrogel material. Antibody release rates were substantially decreased in the lyogel compared to the hydrogel material above a threshold silk concentration. Finally, the material properties of the lyogels were investigated to gain insight into the mechanism of sustained release. In contrast to other hydrogel materials, silk fibroin is a highly hydrophobic molecule. Based on the hydrophobicity of silk and the observed swelling behavior of lyogels, it is hypothesized that rehydration resistance alters the nature of the reversible and irreversible antibody-silk interactions, which govern the rates of sustained release.

Materials and Methods

Materials

Cocoons of *Bombyx mori* silkwork silk were purchased from Tajima Shoji Co., LTD (Sumiyashicho, Naka-Ku, Yokohama, Japan). Purified murine anti-TGFβ IgG1 monoclonal antibody was supplied by Genzyme Corporation (Framingham, MA). Clear Type I borosilicate glass serum vials for lyophilization were obtained from Wheaton Industries, Inc. (Millville, NJ). All chemicals were reagent grade purchased from Sigma-Aldrich (St. Louis, MO) or Mallinckrodt Baker, Inc. (Phillipsburg, NJ). All solutions were prepared using ultra pure water (UPW) with a 18.2 MΩ resistivity and <5 ppb TOC generated by a Millipore Milli-Q Advantage A10 purification system (Billerica, MA).

Lyophilized antibody powders

Antibody solutions at 5 mg mL^{-1} formulated in 20 mM histidine buffer, 0.5 % (w/v) sucrose, pH 6.0 were lyophilized in a LyoStarII tray freeze dryer (FTS Systems, Stone Ridge, NY). Each 5 mL serum vial was filled with 2.5 mL antibody solution and equipped with a vented silicone stopper. Samples were frozen to −45°C and held for 8 hours. Primary drying was performed at −20°C, 100 mTorr for 40 hours. Secondary drying was performed at 35°C, 100 mTorr for 11 hours. At the conclusion of lyophilization, the stoppers were depressed under a vacuum of 600,000 mTorr and the vials were sealed using aluminum tear off caps. Lyophilized antibody samples were stored at 5°C ± 3°C prior to use.

Concentrated silk fibroin solution preparation

Silk fibroin solutions were prepared using an aqueous process described previously [27]. Briefly, removal of the glue-like sericin protein was accomplished by boiling approximately 4 cm^2 silk cocoon pieces in a 0.02 M sodium carbonate solution for 60 minutes. After three ambient UPW rinses, the silk fibroin was air dried at ambient temperature for a minimum of 12 hours. The dried fibroin was solubilized at 20% (w/w) in a 9 M aqueous LiBr solution at

60°C for 60 minutes. This solution was dialyzed against UPW for 48 hours using a 3,500 MWCO Slide-A-Lyzer cassette (Thermo Fisher Scientific Inc., Rockford, IL). Silk concentrations were determined by comparing the mass of solution to the mass of dried silk after storage at 60°C for 12 hours. The silk concentration after dialysis was approximately 7.5% (w/w). Lower concentration silk solutions were prepared by dilution with UPW. Higher concentration silk solutions were prepared by dialysis against 20% (w/v) PEG (10,000 g mol^{-1}) at room temperature at a silk to PEG ratio of 1:33. Silk fibroin solutions were stored at 5°C prior to use.

Preparation of silk hydrogels and lyogels

Silk hydrogels were prepared using the sonication method described previously [37]. Briefly, 8 mL of silk fibroin solution in a 15 mL conical tube was sonicated for 30 s using a Branson 450D sonifier equipped with a 3.175 mm diameter tapered microtip (Branson Ultrasonics Co., Danbury, CT). Sonication power was tailored for each silk concentration from 20% to 65% amplitude to achieve a sol-gel transition within 2 h. The sonicated solutions were cooled to room temperature by immersion in a room temperature water bath. Using a positive displacement pipette, 200 μL of the silk fibroin solution was transferred to a 96 well plate to make a single hydrogel pellet. The plates were allowed to sit at room temperature exposed to air until the solution turned opaque and water droplets formed on the surface, indicating the completion of the sol-gel transition. Lyogels were prepared by lyophilizing the hydrogel containing plates. Aluminum blocks were placed under the plastic plate to maximize heat transfer from the lyophilizer shelf. Lyophilization was carried out according to the parameters described above.

For antibody loaded constructs, lyophilized antibody was added to the cooled solutions to a target concentration of 5 mg·mL^{-1}. The solution was gently inverted to ensure complete dissolution of the antibody powder and homogenous distribution. After thorough mixing, the solution was transferred to plates and allowed to gel as before. Based on this approach, the loading efficiency of antibody in hydrogels was considered 100%.

Swelling properties

Silk lyogels were immersed in phosphate buffered saline (PBS) pH 7.4 at 37°C and sampled at defined time intervals. After removal of excess water by contact with a plastic surface, the weight of the rehydrated lyogel (W_r) was determined. The swelling ratio and fluid recovery were calculated as follows:

$$\text{Swelling ratio} = \frac{W_r - W_d}{W_d}$$

$$\text{Fluid recovery } (\%) = \frac{W_r - W_d}{W_g - W_d} \times 100$$

Where W_d and W_g are the mass of the lyogel and hydrogel respectively.

Fourier transform infrared spectroscopy (FTIR)

Secondary structure of the silk matrix was analyzed by Fourier transform infrared spectroscopy (FTIR) on an MB series spectrometer (ABB Bomem, Quebec, Canada) equipped with a MIRacle attenuated total reflection (ATR) diamond crystal (Pike Technologies, Madison, WI). Data acquisition and analysis were performed using PROTA

(BioTools, Inc., Jupiter, FL) together with RazorTools 6.0 (Spectrum Square Associates, Inc., Ithaca, NY). Each spectrum was collected as a 400 scan interferogram with a 4 cm^{-1} resolution in single-beam mode from 400 to 4000 cm^{-1}. Approximately 3 μL of silk fibroin solution was placed onto the crystal and covered to prevent evaporation. Silk hydrogels and lyogels were pressed onto the crystal using the attached high-pressure clamp equipped concave and flat tips respectively. Protein absorbance spectra in the amide I and amide II regions were obtained by water and water vapor subtraction procedures established previously [41–42].

To quantify secondary structure composition, Fourier self-deconvolution (FSD) of the amide I region (1590–1710) was performed using a Lorentzian peak shape with a half-bandwidth of 25 cm^{-1} and a K factor of 2.0. Contributing bands were identified by second derivative analysis with five point Savitsky-Golay smoothing of the non-FSD spectrum. Manual baseline correction was performed on the FSD spectrum. A maximum entropy Gaussian curve fitting algorithm was executed on the FSD spectrum using peak positions identified in the second derivative $\pm$ 2 cm^{-1}, a maximum peak width of 20 cm^{-1}, and variable peak height. Structural assignment to peak positions was made using wavenumber ranges described by Lu et al. [43]. Structural composition was determined by relative areas of the fit cures.

In vitro antibody release

In vitro antibody release studies were carried out at 37°C in PBS pH 7.4. The hydrogel or lyogel pellets were immersed in 0.5 mL of release medium and stored in a 1.2 mL polystyrene screw top vial. At defined time points each pellet was transferred to a new vial with fresh release medium. The amount of antibody release was determined chromatographically using a protein G ID cartridge (Applied Biosystems, Carlsbad, CA). The bind-elute assay was performed on a 1200 series HPLC (Agilent Technologies, Santa Clara, CA). The binding mobile phase was 0.01 M sodium phosphate, 0.15 M sodium chloride, pH 7.3 and the elution buffer was 0.012 M hydrochloric acid, 0.15 M sodium chloride, pH 2.0 flowing at a rate of 2 mL min^{-1}. Antibody concentrations were calculated by interpolation from a standard curve generated under identical conditions.

Antibody functional stability analysis

Anti-TGFβ antibody functional stability was evaluated in a previously described potency assay based on the TGFβ-induced release of Interleukin-11 (IL-11) by the human lung epithelial cell line A549 [44]. In brief, A549 cells were cultured in Dulbecco's Modified Eagle Medium (DMEM) containing 10% fetal bovine serum (FBS), 1% minimal essential medium (MEM) non-essential amino acids and 1% L-glutamine. A549 cells at approximately 80% confluence were trypsinized and plated into 96-well plates and then incubated 18–24 hours at 37°C in 5% CO_2. On day 2, dilutions of antibody samples were prepared in polypropylene dilution plates. A fixed amount of TGFβ at a concentration of approximately 80% Effective Dose $(ED)_{80}$ was added. Dilution plates were then incubated for 1 hour at 37°C before transferring the contents to corresponding wells of the plates containing the A549 cells. Bioassay plates were then incubated an additional 18–24 hours at 37°C. After incubation, cell supernatants were analyzed using an ELISA assay which detects IL-11 at pg mL^{-1} levels.

The IL-11 ELISA portion of the assay was performed using Nunc-Immuno™ MaxiSorp™ (Nalgene Nunc International, Rochester, NY) plates that were coated with 4 μg mL^{-1} of anti-human IL-11 monoclonal antibody prepared in PBS and incubated overnight at room temperature. ELISA plates were then washed 3× and blocked with 0.5% bovine serum albumin (BSA) in PBS for 1–3 hours at room temperature. After washing again (3×),

standards, controls and cell supernatant were added to the ELISA plates and incubated at room temperature for approximately 2 hours. The ELISA plates were then washed 6× and biotinylated anti-human IL-11 antibody at 0.1 mg mL^{-1} made in sample dilution buffer (0.1% BSA in 1× plate wash buffer) was added. The plates were again incubated for 2 hours at room temperature. After another 6× wash, HRP-streptavidin conjugate at 1:30,000 was added to the wells, incubated for 20 minutes at room temperature and subsequently washed 6×. TMB substrate was then added to the wells and plates were incubated an additional 20 minutes at room temperature while protected from light. The reaction was stopped using 1 N sulfuric acid. Sample absorbance was read at 450 nm on a microplate spectrophotometer (Molecular Devices, Sunnyvale, CA). The IL-11 standard curve analysis was performed using a 4-parameter logistical fit.

Statistical analysis

Unless specified otherwise, each data point is the mean of four trials and is reported ± standard deviation (SD). Where applicable, statistical differences were determined using a two-tailed student's t-test. Differences were considered statistically significant at $p<0.05$.

Results

Swelling properties of silk lyogels

A new procedure was developed to prepare antibody loaded lyophilized silk hydrogels (lyogels) for sustained delivery. Silk lyogels were prepared from 3.2% (w/w) to 12.4% (w/w) silk fibroin solutions. Prior to rehydration the lyogels are rigid white cylinders (Fig. 1 A–D, dry), regardless of silk concentration. Upon rehydration in phosphate buffered saline (PBS), 3.2% (w/w) lyogels rapidly transitioned to a soft, sponge-like texture. Additionally, the low concentration lyogels became more translucent after rehydration (Fig. 1A) with a darker and grayish appearance in the wet 3.2% (w/w) sample. In contrast, lyogels at 6.2% (w/w), 9.2% (w/w), and 12.4% (w/w) (Fig. 1 B–D, wet) maintained a white appearance and remained firm to the touch. To investigate the observed differences in gross morphology, the lyogels were evaluated for swelling and structural properties.

PBS was used as a rehydration medium to simulate physiological conditions. Both fluid mass recovery and the wet mass to dry mass swelling ratio were monitored. PBS uptake occurred rapidly in all samples, reaching an apparent plateau within three days (Fig. 2). Silk lyogels at 3.2% (w/w) recovered approximately 90% of their original hydrogel fluid content (Fig. 2A). Fluid uptake was considerably decreased in lyogels at 6.2% (w/w) and higher, reaching a maximum recovery of 56%. Swelling ratios decreased with increasing silk concentration, with the most significant difference occurring between 3.2% (w/w) and 6.2% (w/w) silk (Fig. 2B). A swelling ratio of 23.1 was observed in 3.2% (w/w) silk lyogels, while 6.2% (w/w), 9.2% (w/w), and 12.4% (w/w) had swelling ratios of 6.7, 4.6, and 3.2, respectively. To further characterize the nature of fluid uptake in silk lyogels, physical measurements were obtained (Fig. 3). Small but significant decreases in cylinder height and diameter were observed after lyophilization. This lyophilization shrinkage effect appeared to increase with increasing silk concentration (Fig. 3). No significant changes in height or diameter were observed upon rehydration of the lyogels.

Structural characterization of silk lyogels

To better understand the differences between silk hydrogels and silk lyogels, secondary structure characterization was performed by FTIR. The infrared (IR) region of 1700–1500 cm^{-1} corresponds to peptide backbone absorption for amide I (1700–1600 cm^{-1}) and amide II (1600–1500 cm^{-1}) bands. Absorbance spectra in this region are used frequently for

determining the secondary structure composition of various proteins, including silk fibroin [41–42].

Fig. 4A shows a typical amide I and amide II FTIR absorbance spectra for 12.4% (w/w) silk solution, hydrogel, and lyogel. No changes in the spectra and structural composition were observed with varying silk concentration from 3.2% (w/w) to 12.4% (w/w) (data not shown). Amide I and II peaks centered at 1643 cm^{-1} and 1545 cm^{-1}, respectively, indicate that the silk solution sample was high in random coil and silk I structures [43]. A shift in IR absorbance to lower wave number was observed upon formation of hydrogels. A strong absorbance signal at 1620 cm^{-1} in the amide I, together with a shift to lower wave number of the amide II, is indicative of a sample rich in β-sheet (silk II) structure [43]. Removal of water through lyophilization had a negligible impact on the appearance of the amide I absorbance spectrum. The amide II band in the lyogel sample shifted to a maximum absorbance at 1515 cm^{-1}. This spectral shift indicates a slight change in the arrangement of β-sheet (silk II) structure upon lyophilization, consistent with the physical shrinkage observed.

Silk structure was characterized further by calculation of secondary structure composition through deconvolution of the amide I band (Fig. 4B). An increase in β-sheet (silk II) composition from 21.9% to 56.9% was observed when the hydrogel sample was compared to silk solution (Fig. 4B). The sol-gel transition was also accompanied by a decrease in random coil (32.1% to 16.6%), turns and bends (22.0% to 11.2%), and silk I (14.3% to 7.2%). Only small changes in secondary structure composition were observed in the lyogel compared to the hydrogel. A slight decrease in β-sheet (silk II) from 56.9% to 52.1% was observed together with a slight increase in random coil from 16.6% to 19.7%.

Suspecting that the predominant β-sheet (silk II) structure may play a role in the hydration properties observed in lyogels, the density of β-sheet (silk II) structure was calculated (Fig. 4C). β-sheet (silk II) density was calculated using the structural composition data in Fig. 5B. The volume of liquid added to form the hydrogel cylinder was used in the β-sheet (silk II) density calculation for silk solutions. Hydrogel and dry lyogel β-sheet (silk II) density were calculated using physical dimension measurements (Fig. 3). Since silk concentration had no impact on structural composition, β-sheet (silk II) density increased in all three forms with increasing silk concentration. Density of β-sheets (silk II) structure was lowest in the cylinder of silk solution, ranging from 6.9 to 27.1 mg (cm^3)$^{-1}$. β-sheet (silk II) density increased dramatically after the transition to hydrogel (17.2 to 67.4 mg (cm^3)$^{-1}$) and increased further after lyophilization (20.0 to 97.5 mg (cm^3)$^{-1}$). The increase in density after lyophilization was caused by a slight shrinking in the physical dimensions of the silk pellet after removal of water.

Antibody release from silk hydrogels and lyogels

In order to evaluate the potential use of the lyogel matrix as a protein delivery system, the retention and release of antibody was compared to the parent hydrogel material. Silk lyogels and hydrogels ranging from 3.2% (w/w) to 12.4% (w/w) loaded with 1 mg antibody at 5 mg mL^{-1} were incubated at 37°C in PBS. The release medium was exchanged at defined time intervals. Collected release medium was assayed for antibody concentration by the protein G-ID method. Antibody release reached a plateau within 11 days at all silk concentrations (Fig. 5A). Cumulative antibody released decreased with increasing silk concentration. Approximately 80% of the antibody was released from the lowest silk concentration (3.2% (w/w)) hydrogels. Cumulative antibody released decreased to 67.5%, 52.5%, and 46.6% for 6.2% (w/w), 9.2% (w/w), and 12.4% (w/w) hydrogels, respectively. The antibody release data was normalized using cumulative release at day 26 as a reference (Fig. 5B). Decreased release rates were observed as a function of increasing silk concentration. At 3.2% (w/w)

silk, complete release was observed after three days. For 6.2% (w/w), 9.2% (w/w), and 12.4% (w/w) the release plateau was reached between 8 and 11 days. Handling of 3.2% (w/w) silk hydrogels proved challenging as the constructs were somewhat brittle and had a tendency to fragment. Hydrogels at 6.2% (w/w) silk and above were not brittle.

Antibody release from the silk lyogels was investigated under identical experimental conditions to silk hydrogels (Fig. 6). At 3.2% (w/w) silk, a rapid release of approximately 70% of total antibody was observed after 15 days (Fig. 6A). A significant decrease in the amount of antibody released was observed at 6.2% (w/w) silk and above. Over the 38 day experiment, only 14.8% of the antibody was released from 6.2% (w/w) and 9.2% (w/w) lyogels. Approximately 10.0% of the antibody was released from 12.4% (w/w) silk lyogels during the same time period. The lyogel antibody release data were also normalized using cumulative release at day 38 as the apparent 100% reference point (Fig. 6B). The normalized release data (Fig. 6B) show that a release plateau was not achieved in 6.2% (w/w), 9.2% (w/w), and 12.4% (w/w) silk lyogels. In the absence of a release plateau, the normalized release rates will decrease slightly as additional antibody is released from the matrices. While the normalized rates of release were comparable between the three higher silk concentration samples, they were substantially decreased compared to the 3.2% (w/w) silk lyogel. Lyophilization did not noticeably impact handling properties of the gels at 6.2% (w/w) silk and above. At 3.2% (w/w) silk, however, lyogels were considerably more robust for handling than their hydrogel counterparts.

Post release antibody functional stability

The quality of protein released from a sustained delivery matrix is of critical importance. As a preliminary indicator of quality, the functional stability of antibody released from silk lyogels was evaluated. Antibody released over the first 48 hours was collected, pooled, and concentrated. Functional stability was assessed by the TGF-β induced IL-11 release assay. Each released antibody sample along with the unincorporated antibody control was assayed in duplicate. Dose response curves depicted in Fig. 7 include the highest and lowest control curve in addition to one curve from each released sample. Curves from the released antibody fell within the range of the control curves for all silk lyogel concentrations. The functional comparability of released versus control antibody was further assessed by the half maximal effective concentration (EC_{50}) values in Table 1. The EC_{50} values for the control sample across four assay instances ranged from 0.483 μg mL^{-1} to 0.587 μg mL^{-1}. Silk lyogel released sample EC_{50} values ranged from 0.462 μg mL^{-1} to 0.554 μg mL^{-1}. The slight decrease in the low EC_{50} values of 3.2% (w/w), 6.2% (w/w) and 9.2% (w/w) relative to the control sample falls within the published accuracy of ±13% for the assay [44].

Discussion

The present work describes the formation and characterization of a silk-based lyogel for the sustained release of monoclonal antibodies. Several features of the lyogel are desirable in a potential sustained release platform for therapeutic proteins. The antibody loaded silk lyogel represents a device in which the therapeutic protein and delivery matrix are manufactured and stored together. This approach is simpler and more convenient, offering an advantage over a delivery system which requires mixing at the point of use [4,5]. The device described here also has three key features that should maximize protein stability. First, the shear and temperature intensive sonication process used to induce the silk sol-gel transition is performed in the absence of antibody. Since this approach is sufficiently gentle to maintain cell viability during encapsulation in silk hydrogels, compatibility with proteins is expected [37]. Once exposure to shear and temperature stresses is eliminated, only the actual sol-gel transition remains as a possible source of destabilizing stress. Second, encapsulation of enzymes in silk has been shown to result in a significant stabilizing effect [39,40]. This

demonstrates that silk as a biomaterial is compatible with protein entrapment, and it is expected this stabilizing effect will extend to antibodies. Finally, the finished product is a lyophilized solid, a highly desirable form to maximize protein stability during long-term storage. In the absence of water, the rates of various chemical reactions that destabilize proteins are reduced to irrelevant timescales [45]. While additional, in-depth, stability characterization needs to be performed; the primary stability end-point was met in this work. Antibody released from silk lyogels was confirmed to maintain biological function in a cell-based bio-assay.

Insight into the physical changes brought about by the lyophilization of hydrogels at various silk concentrations is a critical first step in understanding the nature of the sustained release behavior observed in silk lyogels. The rigid nature of the lyogels is desirable as it would facilitate handling and implantation. A difference was observed in the fluid uptake properties of 3.2% (w/w) silk lyogels compared to higher concentration lyogels. Lyogels at 6.2% (w/w) silk and above showed a resistance to complete rehydration while 3.2% (w/w) silk lyogels rehydrated fully (Fig. 2). The increased swelling ability of the low concentration silk lyogel was consistent with visual observations of the gross morphology (Fig. 1). A lack of physical swelling in the axial or radial directions shows that the cross-linked β-sheet network in lyogels provides a rigid matrix (Fig. 3). Without the possibility of expansion, fluid uptake is limited to the free space available, which will decrease as the concentration of silk fibroin increases. Structural composition differences between hydrogels and lyogels were negligible as determined by FTIR analysis. No changes in composition were found with increasing silk concentration. Silk II (β-sheet) was the primary structural motif in lyogels, accounting for approximately 52% of the structure (Fig. 4). The silk II (β-sheet) arrangement is highly hydrophobic [46]. Considering this hydrophobicity, it appears that the packing density of silk II (β-sheet) structure drives the hydration resistance observed at 6.2% (w/w) silk and above.

The results from the present study imply that primarily hydrophilic/hydrophobic silk-antibody interactions govern antibody release from silk lyogels. Hydration resistance, caused by the hydrophobicity of the silk matrix, provides a secondary means by which silk-antibody interactions can be controlled. Evaluating release behavior from the parent hydrogels demonstrated the effect of silk-antibody interactions. Based on prior work, it is expected that antibodies will exist within the silk matrix in both trapped and untrapped forms [40]. Trapped and untrapped forms result from hydrophilic/hydrophobic interactions that are either reversible (trapped) or irreversible (untrapped) under PBS release conditions. The untrapped form releases rapidly, while the trapped form remains in the matrix until degradation of the silk occurs. Sufficient silk degradation did not occur over the time course of this experiment to impact release of the trapped form. In silk hydrogels, the total amount of trapped antibody increased with increasing silk concentration. This is manifested in Fig. 5A by decreased cumulative antibody release. Additionally, increasing silk concentration decreased the rate of untrapped antibody release. This is seen in Fig. 5B by an increase in the amount of time required to reach the release plateau. These observations show that both reversible and irreversible silk-antibody interactions were enhanced by increasing silk concentration. The enhanced interactions can be attributed to an increase in the number of hydrophobic/hydrophilic contact surfaces as the packing density of silk fibroin increases. While the release rate of untrapped antibody was slower at higher silk concentrations, the overall release was still rapid within 10 days. Based on these results, it appears as though fully swollen silk hydrogels display diffusion-based sustained release limitations similar to those observed in other hydrogel materials [8,47,48].

Antibody release profiles from silk lyogels demonstrated the role of hydration resistance in altering silk-antibody interactions leading to a significantly altered sustained release profile.

Water is primarily excluded from the hydrophobic silk II (β-sheet) secondary structure [43,49]. Removal of water from the amorphous/hydrophilic domains resulted in a slight rearrangement and compacting of the silk II (β-sheet) network based on the shift in the FTIR amide II spectrum (Fig. 4A). Water removal also increased the interactions between silk and antibody molecules. Amorphous domain silk-water interactions were replaced by silk-antibody interactions. These enhanced interactions are expected to decrease release rates for untrapped antibody and/or increase trapped antibody content. Consistent with this hypothesis, removing water from the antibody loaded silk hydrogel constructs dramatically impacted release behavior. A slight decrease in the rate of release (time to plateau Fig. 5B) combined with increase in the amount of trapped (decreased cumulative release Fig. 5A) antibody was observed in 3.2% (w/w) silk lyogels when compared to 3.2% (w/w) hydrogels. Alternatively, release behavior in silk lyogels at 6.2% (w/w) and above was dramatically altered relative to the hydrogels. The rate of release decreased substantially (Fig. 5A), not reaching a plateau during the 38 day experiment. Increasing the silk concentration above 6.2% (w/w) did not alter release profiles further. This threshold release profile behavior is consistent with the significant change in swelling properties between 3.2% (w/w) and 6.2% (w/w) silk lyogels. These observations show that a threshold silk concentration leads to dramatic changes in swelling and release properties, demonstrating that hydration resistance is a critical component of the sustained release observed.

We propose that silk lyogels can be prepared in two forms: low density β-sheet networks (LDBN) and high density β-sheet networks (HDBN). The transition from LDBN to HDBN occurs between 20 mg·$(cm^3)^{-1}$ and 42 mg·$(cm^3)^{-1}$ β-sheet structure in silk lyogels. In the LDBN form, near complete rehydration is observed. In the water rich environment, any enhanced silk-antibody interactions are rapidly reversed, and release behavior comparable to that of the hydrogel is observed (Fig. 8 top). In the HDBN form significant hydration resistance is observed. Lower water content within the HDBN lyogels limits the competition of water with the silk-antibody interactions (Fig. 8 bottom). The decreased kinetics of water-silk interactions replacing antibody-silk interactions results in sustained release of untrapped antibody. These findings indicate that release rates could be controlled by modifying hydration properties of silk lyogels.

Conclusions

A system for the sustained release of pharmaceutically relevant monoclonal antibodies was developed. It is postulated that silk-antibody hydrophobic/hydrophilic interactions are the primary driving force in controlling the sustained release. Hydration resistance in the silk lyogels offers a secondary means through which sustained antibody release can be altered. Hydration resistance was induced in silk lyogels by preparation of a high density β-sheet network. The process used to manufacture silk lyogels does not require the antibody to be exposed to stresses such as shear, temperature, organic solvents, or chemical modification, thus preserving the biological activity of the loaded protein. The avoidance of such stresses should establish a process which is highly compatible with therapeutic proteins with regard to maximizing structural stability and biological function at the therapeutic target. Lyophilization of antibody-loaded silk hydrogels significantly improved long-term antibody release properties over the parent hydrogel material.

Acknowledgments

References

[1]. Piggee C. Therapeutic antibodies coming through the pipeline. Anal Chem 2008;80:2305–10. [PubMed: 18456912]

[2]. Werner RG. Economic aspects of commercial manufacture of biopharmaceuticals. J Biotechnol 2004;113:171–82. [PubMed: 15380655]

[3]. Manabe T, Okino H, Maeyama R, Mizumoto K, Nagai E, Tanaka M, et al. Novel strategic therapeutic approaches for prevention of local recurrence of pancreatic cancer after resection: Trans-tissue, sustained local drug-delivery systems. J Control Release 2004;100:317–30. [PubMed: 15567499]

[4]. Friess W, Uludag H, Foskett S, Biron R. Bone regeneration with recombinant human bone morphogenetic protein-2 (rhbmp-2) using absorbable collagen sponges (acs): Influence of processing on acs characteristics and formulation. Pharm Dev Technol 1999;4:387–96. [PubMed: 10434284]

[5]. Friess W, Uludag H, Foskett S, Biron R, Sargeant C. Characterization of absorbable collagen sponges as rhbmp-2 carriers. Int J Pharm 1999;187:91–9. [PubMed: 10502616]

[6]. Giteau A, Venier-Julienne MC, Aubert-Pouessel A, Benoit JP. How to achieve sustained and complete protein release from plga-based microparticles? Int J Pharm 2008;350:14–26. [PubMed: 18162341]

[7]. Sinha VR, Trehan A. Biodegradable microspheres for protein delivery. J Control Release 2003;90:261–80. [PubMed: 12880694]

[8]. Bhattarai N, Gunn J, Zhang M. Chitosan-based hydrogels for controlled, localized drug delivery. Adv Drug Deliv Rev 2010;62:83–99. [PubMed: 19799949]

[9]. Panyam J, Dali MM, Sahoo SK, Ma W, Chakravarthi SS, Amidon GL, et al. Polymer degradation and in vitro release of a model protein from poly(d,l-lactideco-glycolide) nano- and microparticles. J Control Release 2003;92:173–87. [PubMed: 14499195]

[10]. Quaglia F, Ostacolo L, Nese G, De Rosa G, La Rotonda MI, Palumbo R, et al. Microspheres made of poly(epsilon-caprolactone)-based amphiphilic copolymers: Potential in sustained delivery of proteins. Macromol Biosci 2005;5:945–54. [PubMed: 16208680]

[11]. Vandervoort J, Ludwig A. Preparation and evaluation of drug-loaded gelatin nanoparticles for topical ophthalmic use. Eur J Pharm Biopharm 2004;57:251–61. [PubMed: 15018982]

[12]. Angele P, Abke J, Kujat R, Faltermeier H, Schumann D, Nerlich M, et al. Influence of different collagen species on physico-chemical properties of crosslinked collagen matrices. Biomaterials 2004;25:2831–41. [PubMed: 14962561]

[13]. Gupta P, Vermani K, Garg S. Hydrogels: From controlled release to ph-responsive drug delivery. Drug Discov Today 2002;7:569–79. [PubMed: 12047857]

[14]. Shi W, Ji Y, Zhang X, Shu S, Wu Z. Characterization of ph- and thermosensitive hydrogel as a vehicle for controlled protein delivery. J Pharm Sci. 2010 DOI: 10.1002/jps.22328. in press.

[15]. Solorio L, Zwolinski C, Lund AW, Farrell MJ, Stegemann JP. Gelatin microspheres crosslinked with genipin for local delivery of growth factors. J Tissue Eng Regen Med 2010;4:514–23. [PubMed: 20872738]

[16]. Zheng C, Liang W. A one-step modified method to reduce the burst initial release from plga microspheres. Drug Deliv 2010;17:77–82. [PubMed: 20067365]

[17]. Xu J, Li X, Sun F, Cao P. Pva hydrogels containing beta-cyclodextrin for enhanced loading and sustained release of ocular therapeutics. J Biomater Sci Polym Ed 2010;21:1023–38. [PubMed: 20507706]

[18]. Oh KS, Han SK, Lee HS, Koo HM, Kim RS, Lee KE, et al. Core/shell nanoparticles with lecithin lipid cores for protein delivery. Biomacromolecules 2006;7:2362–7. [PubMed: 16903683]

[19]. Zhu G, Mallery SR, Schwendeman SP. Stabilization of proteins encapsulated in injectable poly (lactide- co-glycolide). Nat Biotechnol 2000;18:52–7. [PubMed: 10625391]

[20]. Dang JM, Leong KW. Natural polymers for gene delivery and tissue engineering. Adv Drug Deliv Rev 2006;58:487–99. [PubMed: 16762443]

[21]. Peppas NA, Bures P, Leobandung W, Ichikawa H. Hydrogels in pharmaceutical formulations. Eur J Pharm Biopharm 2000;50:27–46. [PubMed: 10840191]

[22]. Van Tomme SR, Storm G, Hennink WE. In situ gelling hydrogels for pharmaceutical and biomedical applications. Int J Pharm 2008;355:1–18. [PubMed: 18343058]

[23]. O'Brien FJ, Harley BA, Yannas IV, Gibson L. Influence of freezing rate on pore structure in freeze-dried collagen-gag scaffolds. Biomaterials 2004;25:1077–86. [PubMed: 14615173]

[24]. Maeda H, Sano A, Fujioka K. Profile of rhbmp-2 release from collagen minipellet and induction of ectopic bone formation. Drug Dev Ind Pharm 2004;30:473–80. [PubMed: 15244082]

[25]. Bigi A, Cojazzi G, Panzavolta S, Roveri N, Rubini K. Stabilization of gelatin films by crosslinking with genipin. Biomaterials 2002;23:4827–32. [PubMed: 12361622]

[26]. Charulatha V, Rajaram A. Influence of different crosslinking treatments on the physical properties of collagen membranes. Biomaterials 2003;24:759–67. [PubMed: 12485794]

[27]. Kim UJ, Park J, Li C, Jin HJ, Valluzzi R, Kaplan DL. Structure and properties of silk hydrogels. Biomacromolecules 2004;5:786–92. [PubMed: 15132662]

[28]. Matsumoto A, Chen J, Collette AL, Kim U-J, Altman GH, Cebe P, et al. Mechanisms of silk fibroin sol-gel transitions. J Phys Chem B 2006;110:21630–8. [PubMed: 17064118]

[29]. Inoue S, Tanaka K, Arisaka F, Kimura S, Ohtomo K, Mizuno S. Silk fibroin of bombyx mori is secreted, assembling a high molecular mass elementary unit consisting of h-chain, l-chain, and p25, with a 6:6:1 molar ratio. J Biol Chem 2000;275:40517–28. [PubMed: 10986287]

[30]. Panilaitis B, Altman GH, Chen J, Jin HJ, Karageorgiou V, Kaplan DL. Macrophage responses to silk. Biomaterials 2003;24:3079–85. [PubMed: 12895580]

[31]. Horan RL, Antle K, Collette AL, Wang Y, Huang J, Moreau JE, et al. In vitro degradation of silk fibroin. Biomaterials 2005;26:3385–93. [PubMed: 15621227]

[32]. Wang Y, Rudym DD, Walsh A, Abrahamsen L, Kim HJ, Kim HS, et al. In vivo degradation of three-dimensional silk fibroin scaffolds. Biomaterials 2008;29:3415–28. [PubMed: 18502501]

[33]. Yucel T, Cebe P, Kaplan DL. Vortex-induced injectable silk fibroin hydrogels. Biophys J 2009;97:2044–50. [PubMed: 19804736]

[34]. Zhang YQ, Zhou WL, Shen WD, Chen YH, Zha XM, Shirai K, et al. Synthesis, characterization and immunogenicity of silk fibroin-l-asparaginase bioconjugates. J Biotechnol 2005;120:315–26. [PubMed: 16102867]

[35]. Aramwit P, Kanokpanont S, De-Eknamkul W, Srichana T. Monitoring of inflammatory mediators induced by silk sericin. J Biosci Bioeng 2009;107:556–61. [PubMed: 19393558]

[36]. Meinel L, Hofmann S, Karageorgiou V, Kirker-Head C, McCool J, Gronowicz G, et al. The inflammatory responses to silk films in vitro and in vivo. Biomaterials 2005;26:147–55. [PubMed: 15207461]

[37]. Wang X, Kluge JA, Leisk GG, Kaplan DL. Sonication-induced gelation of silk fibroin for cell encapsulation. Biomaterials 2008;29:1054–64. [PubMed: 18031805]

[38]. Leisk GG, Lo TJ, Yucel T, Lu Q, Kaplan DL. Electrogelation for protein adhesives. Adv Mater 2010;22:711–5. [PubMed: 20217775]

[39]. Lu S, Wang X, Lu Q, Hu X, Uppal N, Omenetto FG, et al. Stabilization of enzymes in silk films. Biomacromolecules 2009;10:1032–42. [PubMed: 19323497]

[40]. Qiang L, Xiaoqin W, Xiao H, Peggy C, Fiorenzo O, David LK. Stabilization and release of enzymes from silk films. Macromol Biosci 2010;10:359–68. [PubMed: 20217856]

[41]. Dong A, Huang P, Caughey WS. Protein secondary structures in water from second-derivative amide i infrared spectra. Biochemistry 1990;29:3303–8. [PubMed: 2159334]

[42]. Dong A, Prestrelski SJ, Allison SD, Carpenter JF. Infrared spectroscopic studies of lyophilization- and temperature-induced protein aggregation. J Pharm Sci 1995;84:415–24. [PubMed: 7629730]

[43]. Lu Q, Hu X, Wang X, Kluge JA, Lu S, Cebe P, et al. Water-insoluble silk films with silk i structure. Acta Biomater 2010;6:1380–7. [PubMed: 19874919]

[44]. Rapoza ML, Fu D, Sendak RA. Development of an in vitro potency assay for therapeutic tgf[beta] antagonists: The a549 cell bioassay. J Immunol Methods 2006;316:18–26. [PubMed: 17010369]

[45]. Chang LL, Pikal MJ. Mechanisms of protein stabilization in the solid state. J Pharm Sci 2009;98:2886–908. [PubMed: 19569054]

[46]. Koide S, Huang X, Link K, Koide A, Bu Z, Engelman DM. Design of single-layer beta-sheets without a hydrophobic core. Nature 2000;403:456–60. [PubMed: 10667801]

[47]. Teles H, Vermonden T, Eggink G, Hennink WE, de Wolf FA. Hydrogels of collagen-inspired telechelic triblock copolymers for the sustained release of proteins. J Control Release. 2010

[48]. Mandal BB, Kapoor S, Kundu SC. Silk fibroin/polyacrylamide semi-interpenetrating network hydrogels for controlled drug release. Biomaterials 2009;30:2826–36. [PubMed: 19203791]

[49]. Wang X, Yucel T, Lu Q, Hu X, Kaplan DL. Silk nanospheres and microspheres from silk/pva blend films for drug delivery. Biomaterials 2010;31:1025–35. [PubMed: 19945157]
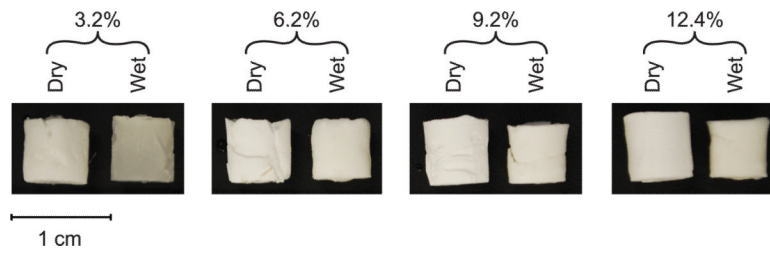
Figure 1.
Lyogels at varying silk concentrations prior to (dry) and after rehydration (wet).
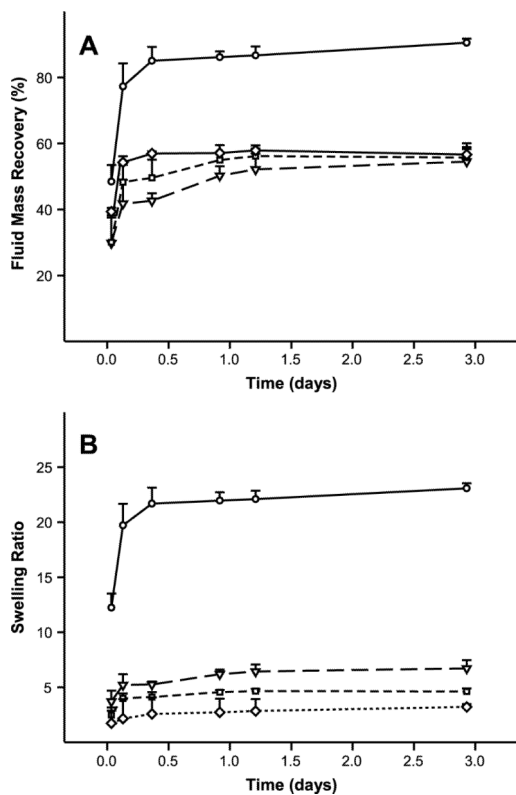
Figure 2.
Swelling properties of silk lyogels. (A) Fluid mass recovery and (B) swelling ratio for 3.2% (circles, solid line), 6.2% (triangle, long dashed line), 9.2% (square, short dashed line), and 12.4% (diamonds, dotted line) silk lyogels. Lines were added as a visual aid.
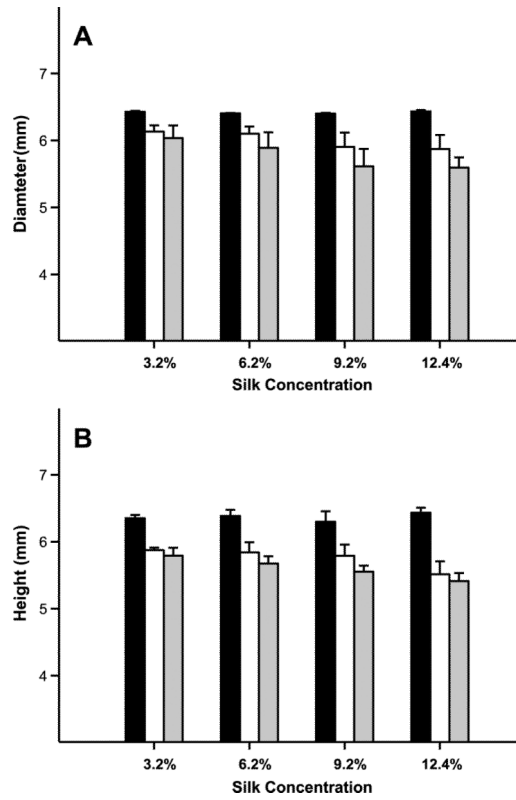
Figure 3.
Physical dimensions of silk hydrogel and lyogel pellets measured by a micro caliper at
varying silk concentrations. (A) Diameter and (B) height measurements for sonication
induced hydrogels (black bars), lyogels (white bars), and rehydrated lyogels (gray bars).
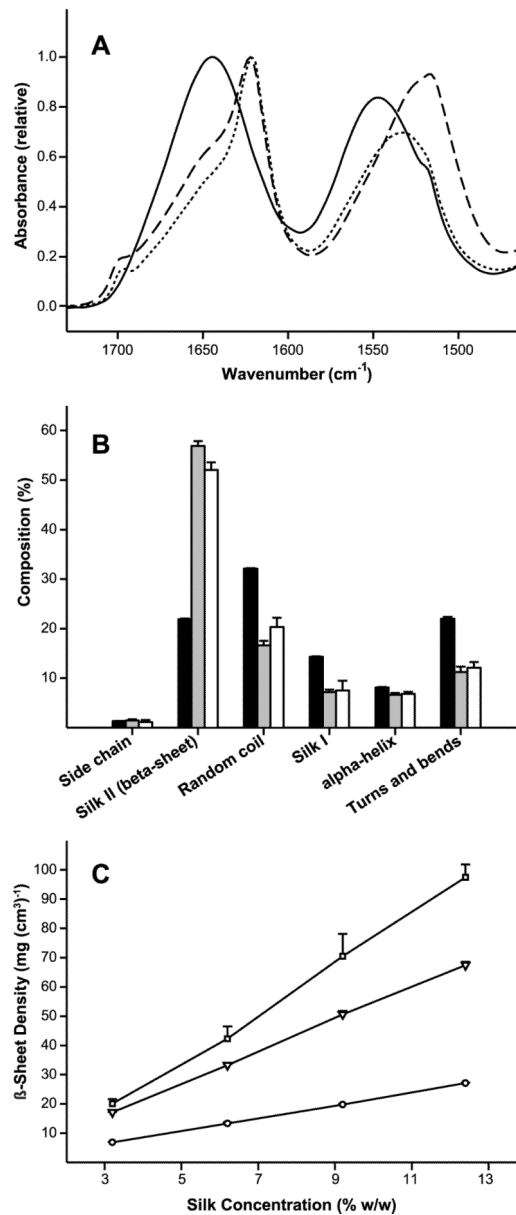
Figure 4.
Structural characterization of silk lyogel constructs. (A) Normalized FTIR absorbance spectra (amide I and amide II bands) after buffer and water vapor subtraction comparing 12.4% (w/v) silk solution (solid line), sonication induced hydrogel (dotted line), and lyogel (dashed line). (B) Secondary structure composition determined by deconvolution of the FTIR amide I absorbance band for 12.4% (w/v) silk solution (black bars), sonication induced hydrogels (gray bars), and lyogels (white bars). (C) Calculated β-sheet density as a function of silk concentration for solution (circles, solid line), sonication induced hydrogels (triangles, long dashed line), and lyogels (squares, short dashed line). Where error bars are not visible, they fall within the background. Lines were added as a visual aid.
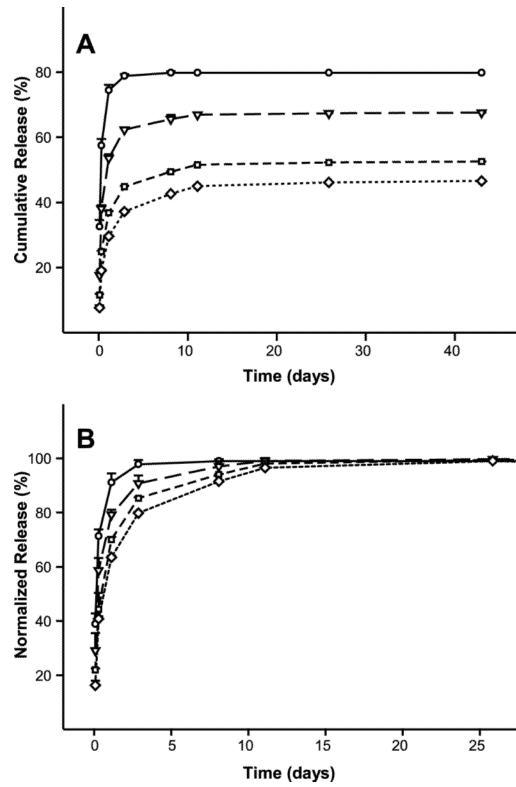
Figure 5.
Antibody release from sonication induced hydrogels at varying silk concentrations, 3.2% (circles, solid line), 6.2% (triangles, long dashed line), 9.2% (square, short dashed line), and 12.4% (diamonds, dotted line). (A) Cumulative release as a function of time. (B) Cumulative release normalized to 100% at the release plateau from day 25 to day 43. Where error bars are not visible, they fall within the symbol. Lines were added as a visual aid.
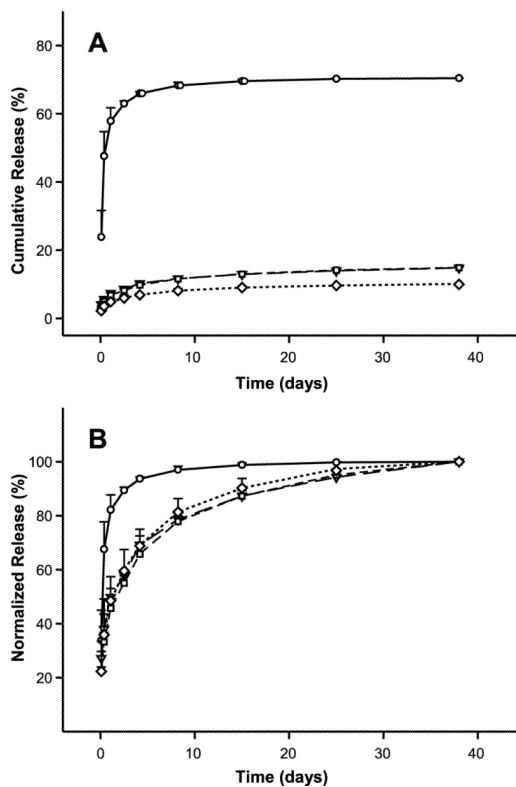
Figure 6.
Antibody release from lyogels at varying silk concentrations, 3.2% (circles, solid line), 6.2% (triangles, long dashed line), 9.2% (squares, short dashed line), and 12.4% (diamonds, dotted line). (A) Cumulative release as a function of time. (B) Cumulative release normalized to 100% at day 38. Where error bars are not visible, they fall within the symbol. Lines were added as a visual aid.
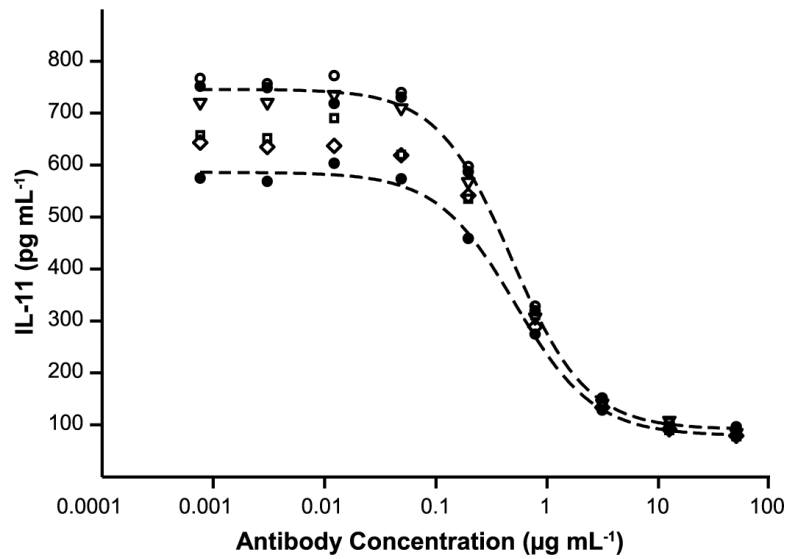
Figure 7.
Representative IL-11 inhibition dose response curves comparing functional behavior of nonencapsulated antibody to antibody released from varying concentration silk lyogels. Filled circles and dashed line four parameter fits represent the lowest and highest nonencapsulated control antibody responses from n=4 trials. Empty symbols represent one response curve from n=2 trials for 3.2% (circle), 6.2% (triangle), 9.2% (square) and 12.4% (diamond) lyogels.
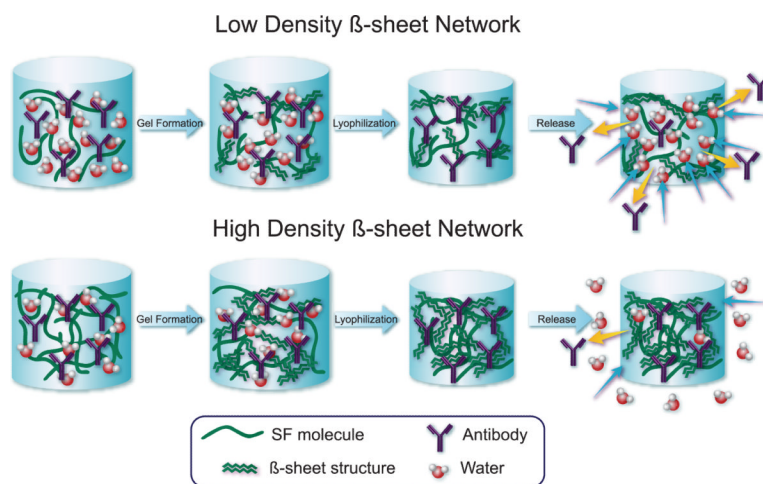
Figure 8.
Schematic representation of water uptake and antibody release behavior for low (~20 mg $(cm^3)^{-1}$) and high (>35 mg $(cm^3)^{-1}$ β-sheet density silk lyogels. Removal of water by lyophilization leads to increased silk-antibody interactions. Interactions are more numerous in the high density β-sheet samples, trapping a larger fraction of antibody. Increased hydrophobicity of the high density β-sheets also retards water uptake, decreasing swelling and antibody release.

Table 1

Range of EC_{50} values obtained from multiple IL-11 inhibition assay instances. For the control sample n=4, while for the released antibody samples n=2.

Sample	EC_{50} Low (µg mL^{-1})	EC_{50} High (µg mL^{-1})
Control	0.483	0.587
Antibody from 3.2% lyogel	0.469	0.513
Antibody from 6.2% lyogel	0.462	0.480
Antibody from 9.2% lyogel	0.465	0.554
Antibody from 12.4% lyogel	0.518	0.551